Destruction of Stearic Acid Nitroxyl Radicals Mediated by Photoexcited Merocyanine 540 in Liposomal and Micellar Systems†

Maryse Hoebeke,* Alain Seret, Jacques Piette, and Albert Van de Vorst

Laboratory of Experimental Physics, Institute of Physics B5, University of Liège, B-4000 Liege, Belgium

Received July 21, 1992; Revised Manuscript Received December 29, 1992

ABSTRACT: Fatty acid spin labels have been included into liposomes and micelles, in order to study the photochemical behavior of merocyanine 540 toward nitroxyl radicals situated at various depths in the bilayer or the surfactant layer. Visible illumination of the dye, either free in ethanol or bound to liposomes or micelles, leads to the reduction of the electron spin resonance signal of the label. The efficiency of the interaction between merocyanine 540 and spin labels depends on the depth at which the nitroxyl moiety is localized in the micelle or vesicle. Fluorescence measurements indicate that the first excited singlet state of merocyanine 540 is not directly implicated in the reaction mechanism. Flash photolysis experiments conducted in aqueous solutions of hexadecyltrimethylammonium bromide micelles show that the presence of nitroxyl radical decreases the rate constant of triplet decay in a concentration-dependent fashion. The corresponding quenching rate constant (k_q) is determined for the different spin labels. The k_q values and the reduction rates of ESR signal show the same dependence on the localization of the nitroxyl moiety in the micelles.

Merocyanine 540 (MC540)[1] is a lipophilic and anionic dye showing great promise as a photosensitizer for selective killing of occult tumor cells in autologous emission bone marrow grafts (Sieber et al., 1986), elimination of leukemic cells (Sieber et al., 1987a) and sterilization of blood products (Sieber et al., 1987b). Previous studies have indicated that visible light irradiation of MC540, either free in ethanol or bound to intact cells or liposomes, does not lead to the generation of singlet oxygen in appreciable yield, the major photoprocesses being photoisomerization and fluorescence (Aramendia et al., 1988; Hoebeke et al., 1988, 1991; Davila et al., 1989). Interestingly, the MC540 photoisomerization and fluorescence quantum yields are strongly dependent on the viscosity of the medium, whereas the singlet oxygen quantum yield remains unchanged whatever the solvent viscosity (Hoebeke et al., 1990).

At the present time, the photodynamic therapeutic activity of the dye is associated either with singlet oxygen formation (Sieber et al., 1986; Kalyanaraman et al., 1987) or with localized disruption of neoplastic cells due to efficient photoisomerization of lipid-bound MC540 (Davila et al., 1989). However, in addition to these photophysical processes, it has been reported that liposome bound MC540 can also initiate oxidation–reduction (Type 1) photoreactions (Feix & Kalyanaraman, 1991). In MC540-treated cells irradiated with visible light, the relative weight of Type 1 (radical-involving) and Type 2 (singlet oxygen-involving) processes should depend on oxygen concentration. Type 1 mechanisms have been shown to trigger, for example, membrane component modifications such as formation of lipid alkyl (Pryor, 1976; Ferradini, 1986). The examination of a Type 1 reaction mediated by MC540 is thus an important step in understanding the molecular basis of the sensitivity of leukemic cells to the photosensitizing effect of MC540.

The MC540 binding to liposomes and the state of MC540 aggregation in these membrane mimetic structures are rather complex. A monomer–dimer equilibrium exists within the lipid bilayer membrane, generating a 5-fold excess of MC540 monomers oriented parallel to the phospholipid chains, with their sulfonated group probably near the membrane surface, over those oriented in the perpendicular direction (Verkman, 1987). MC540 dimers are located deeply in the membrane, perpendicular to the phospholipid chains. Both monomers and dimers can also undergo translocation phenomena leading them to the opposite bilayer of the membrane (Verkman, 1987). Therefore, because MC540 monomers and dimers are located at different sites within the lipid membrane, it is worth studying in details the photochemical behavior of MC540 molecules in terms of the depth and the monomer–dimer equilibrium in the lipid membrane. Stearic acids labeled with a nitroxide spin probe at different positions along the carbon chain are useful probes in such studies of oxidation–reduction reactions in organized systems (Melhorn & Packer, 1982; 1984; Chen et al., 1989).

In this work, four spin-labeled stearic acids (*n*-DSA) having their nitroxyl group at various positions (C_5, C_7, C_{12}, and C_{16})

† M.H. is senior research assistant and J.P. is senior research associate from the Belgium National Fund for Scientific Research (NFSR, Brussels, Belgium). This work was granted by the NFSR and NFMSR (Convention 3′ 4589'90).

* Corresponding author.

[1] Abbreviations: k_q, quenching rate constant of merocyanine 540 triplet by nitroxyl radical; ESR, electron spin resonance; MC540, merocyanine 540; *n*-DSA, *n*-doxyl stearic acid spin probe; DMPC, dimyristoyl-L-α-phosphatidylcholine; carbamoyl, 3-carbamoyl-2,2,5,5-tetramethyl-3-pyrrolin-1-yloxy; TEMPO, 2,2,6,6-tetramethyl-1-piperidinyloxy; C_{16}TAB, hexadecyltrimethylammonium bromide; C_{14}TAB, tetradecyltrimethylammonium bromide; C_{12}TAB, dodecyltrimethylammonium bromide; NADPH, reduced nicotinamide adenine dinucleotide phosphate; 5-DSA, 2-(3-carboxypropyl)-4,4-dimethyl-2-tridecyl-3-oxazolidinyloxy; 7-DSA, 2-(5-carboxypentyl)-4,4-dimethyl-2-undecyl-3-oxazolidinyloxy; 12-DSA, 2-(10-carboxydecyl)-2-hexyl-4,4-dimethyl-3-oxazolidinyloxy; 16-DSA, 2-(14-carboxytetradecyl)-2-ethyl-4,4-dimethyl-3-oxazolidinyloxy; MLV, multilamellar large vesicle; [M], micelle concentration; cmc, critical micelle concentration; N, mean aggregation number; τ_c, correlation time parameter; W_0, central line width at half-height; h_0, amplitude of the center line; h_{-1}, amplitude of the high-field line; S, order parameter; $T'_{\parallel}$ and $T'_{\perp}$, anisotropic hyperfine splittings; τ_I, photoisomer lifetime; τ_T, triplet lifetime; k_T, triplet decay rate constant; ^{3}MC, MC540 triplet state; $MC^{\bullet -}$, MC540 radical anion; $MC^{\bullet +}$, MC540 radical cation.

0006-2960/93/0432-2730$04.00/0

along the carbon chain have been incorporated into dimyristoyl-L-α-phosphatidylcholine (DMPC) large unilamellar liposomes. They have allowed us to determine which MC540 molecule can be responsible for a Type 1 photoreaction. Moreover, the efficiency of the Type 1 photoreaction between MC540 and the nitroxyl group has been examined as a function of the probe depth in the bilayer. Because of the simultaneous presence of MC540 monomers and dimers and the possible folding of the stearic acid chain (Feix et al., 1984), the interpretation of the results obtained with the liposome system requires comparison with a simpler organized system. Cationic micelles of different size have been chosen. In these micelles, MC540 is solubilized predominantly as a monomer (Dodin et al., 1987) and the folding of the stearic acid chain can be controlled using appropriate surfactant chain length (Baglioni et al., 1990a,b).

EXPERIMENTAL PROCEDURES

Chemicals. MC540 was obtained from Eastman Kodak Co. (Rochester, NY); absolute ethanol was from Merck (Darmstadt, Germany); chloroform was from Union Chimique Belge (Brussels, Belgium); 3-carbamoyl-2,2,5,5-tetramethyl-3-pyrrolin-1-yloxy (carbamoyl), 2,2,6,6-tetramethyl-1-piperidinyloxy, (TEMPO), hexadecyltrimethylammonium bromide (C_{16}TAB), tetradecyltrimethylammonium bromide (C_{14}TAB), and dodecyltrimethylammonium bromide (C_{12}TAB) were from Aldrich (Milwaukee, WI); dimyristoyl-L-α-phosphatidylcholine (DMPC) and reduced nicotinamide adenine dinucleotide phosphate (NADPH) were from Sigma (St. Louis, MO). Potassium hexacyanoferrate(III) was supplied by J. T. Baker Chemical Co. (Amsterdam, The Netherlands). The doxyl stearic acid spin probes (Aldrich) were 2-(3-carboxypropyl)-4,4-dimethyl-2-tridecyl-3-oxazolidinyloxy (5-DSA), 2-(5-carboxypentyl)-4,4-dimethyl-2-undecyl-3-oxazolidinyloxy (7-DSA), 2-(10-carboxydecyl)-2-hexyl-4,4-dimethyl-3-oxazolidinyloxy (12-DSA), and 2-(14-carboxytetradecyl)-2-ethyl-4,4-dimethyl-3-oxazolidinyloxy (16-DSA).

Liposome Preparation. DMPC (5 mg/mL) and spin-labeled stearic acids were dissolved together in chloroform and the solutions were dried under vacuum in a rotary evaporator. Multilamellar large vesicles (MLV) were obtained by mechanical stirring (vorter mixer) of the lipid film suspended in phosphate buffer (pH 7.0) at temperature above the DMPC phase-transition temperature (23 °C; Chapman, 1967). After hydration, five cycles of freeze–thawing procedure using liquid nitrogen were carried out to improve incorporation of labeled stearic acid into the liposome phospholipid bilayer. The suspension was then transferred into an extruder (Lipex Biomembrane, Vancouver, Canada) which allows its filtration through polycarbonate filters (0.1-μm pore size, Nucleopore Corp., Pleasanton, CA) employing pressure of up to 6895 Pa of nitrogen gas (Hope et al., 1985). This extrusion was carried out above the phase-transition temperature of the phospholipids and was repeated 10 times. This technique allows us to obtain unilamellar liposomes whose mean size is about 90-nm diameter and whose polydispersity is very low (Nayer & Schroit, 1985; Mayer et al., 1986). The concentration of spin-labeled stearic acid was approximately 7.4×10^{-5} M and the molar ratio of label to lipid was 0.01. Spin-labeled liposomes were incubated for 20 min at 30 °C with MC540 solution (5×10^{-5} M). Considering the molar ratio between phospholipid and MC540 (higher than 73), the concentration of MC540 molecules in water, unbound to liposomes, can be considered as negligible (Sikurova et al., 1989).

Micelle Concentration Determination. The micelle concentration [M] was calculated by use of the classical relation

$$[M] = \frac{[\text{surfactant}] - \text{cmc}}{N}$$

where cmc stands for the critical micelle concentration and N for the mean aggregation number. The following data were used: $N = 80$ and cmc $= 9.4 \times 10^{-4}$ M for C_{16}TAB, $N = 70$ and cmc $= 3.7 \times 10^{-3}$ M for C_{14}TAB (Abu Handiyyah & Kumari, 1990), and $N = 53$ and cmc $= 1.5 \times 10^{-2}$ M for C_{12}TAB (Imae et al., 1986; Zielinski et al., 1989),

Electron Spin Resonance Measurements. ESR spectra were run on a Varian E109 or a Bruker ESP 300E spectrometer working in the X-band range and equipped with a temperature control accessory. All measurements concerning the liposomes were made at 31 °C and the temperature was controlled directly inside the microwave cavity with a Fluke 51 thermometer. Spectra were recorded by using a 100-G scan range at 10-mW microwave power and 2-G modulation amplitude. The labeled liposomes suspension was introduced into a 50-μL capillary tube for ESR measurements. For the micellar and ethanolic solutions, an ESR liquid flat cell was used. The spin labels used in our experiments were only sparingly soluble in water but were readily solubilized by the micelle solutions, so a reasonable assumption was that the labels are associated with the micelles (Bales & Kevan, 1982; Abu-Hamdiyyah & Kumari, 1990).

The spectra of 5-, 7-, 12- and 16-DSA spin labels in DMPC liposomes were qualitatively identical with those previously published in the literature (Figure 1) (Dousset et al., 1986; Takahashi et al., 1988; Chen et al., 1988). The spectrum of 12-DSA in water is given in Figure 1C. The comparison with the spectrum of the same label in the bilayers led us to conclude that the amount of water free spin label was very low under our experimental conditions.

In the bilayers, the four spin labels were oriented with their long axes parallel to the phospholipid chains, yielding informations on the environment of the C_5, C_7, C_{12}, and C_{16} carbons, respectively (Jost et al., 1971). For the stearic acids labeled on C_{12} and C_{16}, which were the less immobilized probes, their motions were compared in terms of the empirical correlation time parameter τ_c, defined as

$$\tau_c = (6.5 \times 10^{-10}) W_0 [(h_0/h_{-1})^{1/2} - 1]$$

where W_0 is the width of the central line at half-height and h_0 and h_{-1} are the amplitudes of the center- and high-field lines, respectively (Henry & Keith, 1971). The τ_c values obtained were 2.2×10^{-9} and 0.85×10^{-9} s for 12-DSA and 16-DSA, respectively. For the spin labels undergoing rapid anisotropic motions (5-DSA and 7-DSA), the order parameter S was calculated with the use of the formula

$$S = \frac{2T'_{\parallel} - 2T'_{\perp}}{2T_{\parallel} - 2T_{\perp}}$$

where $T'_{\parallel}$ and $T'_{\perp}$ are the anisotropic hyperfine splitting measured from the ESR spectra and $2T_{\parallel} - 2T_{\perp} = 52$ G (Hubbel & Mc Connel, 1971). S values of 0.615 and 0.576 were obtained for 5-DSA and 7-DSA, respectively. All measured correlation times and order parameters were in good agreement with those available in the literature (Hubbel et al., 1971; Yoshiska, 1978). Moreover, they were not significantly modified by the presence of MC540 under our experimental conditions.

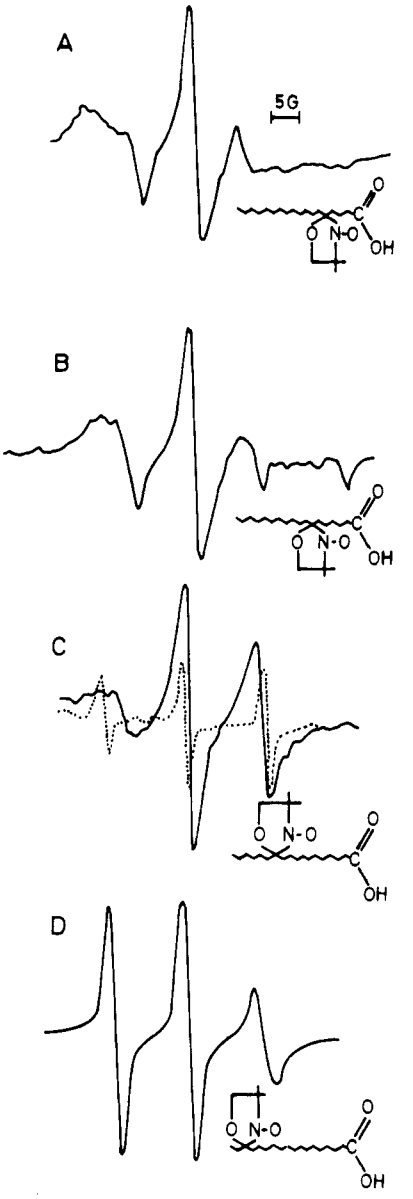

FIGURE 1: ESR spectra (solid line) at 31 °C of (A) 5-DSA, (B) 7-DSA, (C) 12-DSA, and (D) 16-DSA in DMPC liposomes. In panel C, the dotted line is the 12-DSA spectrum in the aqueous phase.

All the nitroxide concentrations were measured by double integration of the ESR spectra and calibrated against a standard solution of carbamoyl. Then, the peak heights were correlated with the concentration of nitroxides. Nitrogen bubbling was used to eliminate oxygen from the different solutions. Irradiation of the samples was performed inside the microwave cavity with light from a slide projector (Pradovit RA 150, Leitz, Germany), filtered by a cutoff filter (OG515, Schott, Germany) in order to eliminate light under 500 nm.

Fluorescence Measurements. The fluorescence measurements were carried out on an SLM-Aminco 500 spectrofluorometer (SLM Instruments Inc.).

Flash Photolysis Experiments. The flash photolysis apparatus and the method for N_2 saturation of the samples have been described elsewhere (Seret & Van de Vorst, 1990). In each experiment, the outer jacket of the photolysis cell was filled with a filter solution made of 0.21 M $CuCl_2$ and 1.06 M $CaCl_2$ aqueous solution which removes wavelengths below 380 nm and above 700 nm (Hoebeke et al., 1988). The errors on the excited-state lifetimes and the quenching rate constants

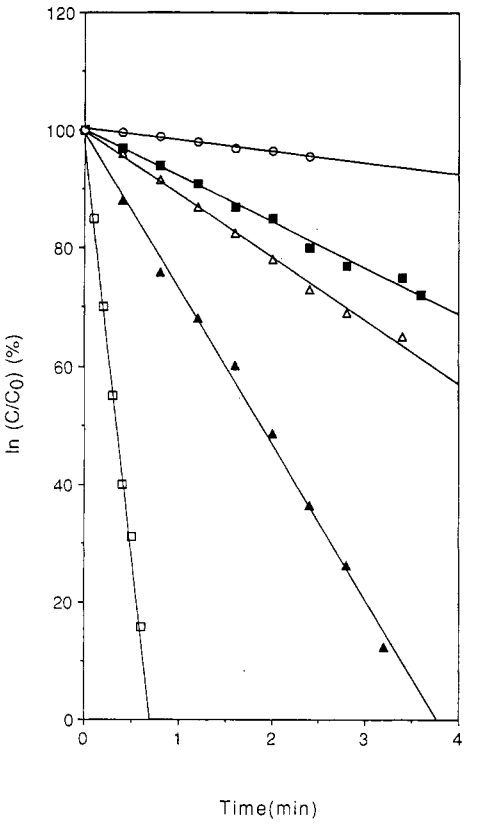

FIGURE 2: Decrease of the *n*-DSA concentration, by photoexcited MC540 (5×10^{-5} M), as a function of the illumination time. The samples were bubbled with nitrogen. (○) 16-DSA in ethanolic solution; (■) 12-DSA, (△) 7-DSA, (▲) 16-DSA, and (□) 5-DSA, incorporated in DMPC liposomes (31 °C). C and C_0 (7.4×10^{-5} M) are the nitroxide concentrations during the irradiation and the nitroxide concentration before irradiation, respectively.

k_q are estimated to be 5% and 10%, respectively (Seret & Van de Vorst, 1990).

RESULTS

Photodestruction of Nitroxide Stearic Spin Labels in Ethanol or Incorporated in Liposomes. The interaction between MC540 and n-DSA was first examined in ethanol, in order to compare the rates of *n*-DSA ESR signal decay in a homogeneous solvent. The ESR spectra of the stearic acid spin probes (5-DSA, 7-DSA, 12-DSA, and 16-DSA) dissolved in ethanol consisted of three symmetric absorption lines and was not affected by the addition of MC540. In a N_2-saturated ethanol solution containing 5×10^{-5} M MC540 and 7×10^{-5} M *n*-DSA, the onset of irradiation caused a slow decrease of the amplitude of the spin label signal, the shape of the spectrum being unchanged. The decay rate was identical for the four labels in N_2- and N_2O-saturated solutions and was found to be first-order dependent on MC540 concentration (from 5×10^{-5} to 10^{-3} M). It was 3-fold increased when the temperature was raised from 31 to 40 °C. In the absence of MC540, the irradiation has generated no variation of the *n*-DSA signal amplitude.

In the presence of 5×10^{-5} M MC540, the ESR signal amplitude of *n*-DSA incorporated in liposomes was destroyed by irradiation (Figure 2) with no observable modification of the shape of the ESR spectra. The destruction rates followed first-order kinetics. They were identical in N_2- and N_2O-saturated solutions but depended on *n*-DSA used. As shown in Figure 2, the photodestruction rates are in the following order: 5-DSA > 16-DSA > 7-DSA > 12-DSA. When the

spin label to lipid ratio was increased, the characteristic nitroxide liquid lines originating from the probe free in solution could be detected (Figure 1C). This observation indicated that, under our experimental conditions, a maximal spin label uptake in the liposomes was reached. No reduction of the intensity of these liquid lines was initiated by the irradiated MC540 embedded in liposomes, showing that, under these conditions, MC540 was not able to destroy the spin labels situated in the outer aqueous phase. ESR spectra remained unchanged when spin labels incorporated in liposomes were irradiated in the absence of MC540 or when liposomal solutions labeled with spin labels and MC540 were not irradiated. These results clearly indicated that photoexcited MC540 was able to destroy the nitroxide group attached to stearic acid incorporated in liposome. They also showed that the destruction rate depends strongly on the position of the nitroxide in the membrane layer. Moreover, the absence of a N_2O effect seemed to rule out the possibility of electron ejection by photoexcited MC540 and subsequent capture by the nitroxyl radical. In order to further characterize the mechanism of the photochemical process, it appeared necessary to determine (i) which of the MC540 excited states (first singlet or triplet) was the reactive intermediate in the photodestruction reaction and (ii) whether or not the efficiency of this photodestruction was identical at various depths in the lipid bilayer. Fluorescence, flash photolysis, and other ESR experiments were undertaken using positively charged micelles, which provide a simple model of well-organized hydrophobic structures, in order to bring an answer to these questions.

With regard to the fluorescence, the shape, the wavelengths, and the intensity of the emission spectrum of MC540 in ethanol were unaffected by the addition of up to 10^{-2} M *n*-DSA. These observations would rule out any direct participation of the first excited singlet state in the destruction of *n*-DSA mediated by photoexcited MC540.

Flash Photolysis in C_{16}TAB Micelles. Flash photolysis experiments were performed in order to investigate the role of the MC540 triplet state in the studied reaction mechanism. They were conducted in C_{16}TAB micellar aqueous solutions because *n*-DSA are oriented parallel to the amphiphilic components of these micelles (Bales & Kevan, 1982) and MC540 molecules are incorporated predominantly in the C_{16}TAB micelles as monomers (Dodin et al., 1987). Flash excitation of N_2-saturated aqueous solutions of 10^{-2} M C_{16}TAB and MC540 led to the observation of two transient absorption bands with different decay rates. The faster decaying band extended from 640 to 700 nm and presented a maximum at 670 (Figure 3A), and the slower extended from 470 to 640 nm and showed a maximum at 565 nm (Figure 3B). The two bands exhibited their maximal amplitude immediately after the flash. In aerated solutions, the broad transient absorption observed above 640 nm disappeared. According to previous investigations (Hoebeke et al., 1988; Aramendia et al., 1988; Seret et al., 1990), this band was assigned to the MC540 triplet state and the 470–640-nm band to the MC540 photoisomer. The photoisomer decay was monitored at 600 nm in order to be outside the ground-state absorption band and the triplet decay was followed at 680 nm in order to be outside the end tail of the photoisomer absorption spectrum. They both followed first-order kinetics characterized by a lifetime $\tau_I = 4.3$ ms (24.5 °C) for the photoisomer and $\tau_T = 2.3$ ms for the triplet state. To study the influence of an electron donor or an electron acceptor on MC540 oxidation–reduction chemistry, the influence of the addition of NADPH or K_3FeCN_6 on the MC540 triplet lifetime was

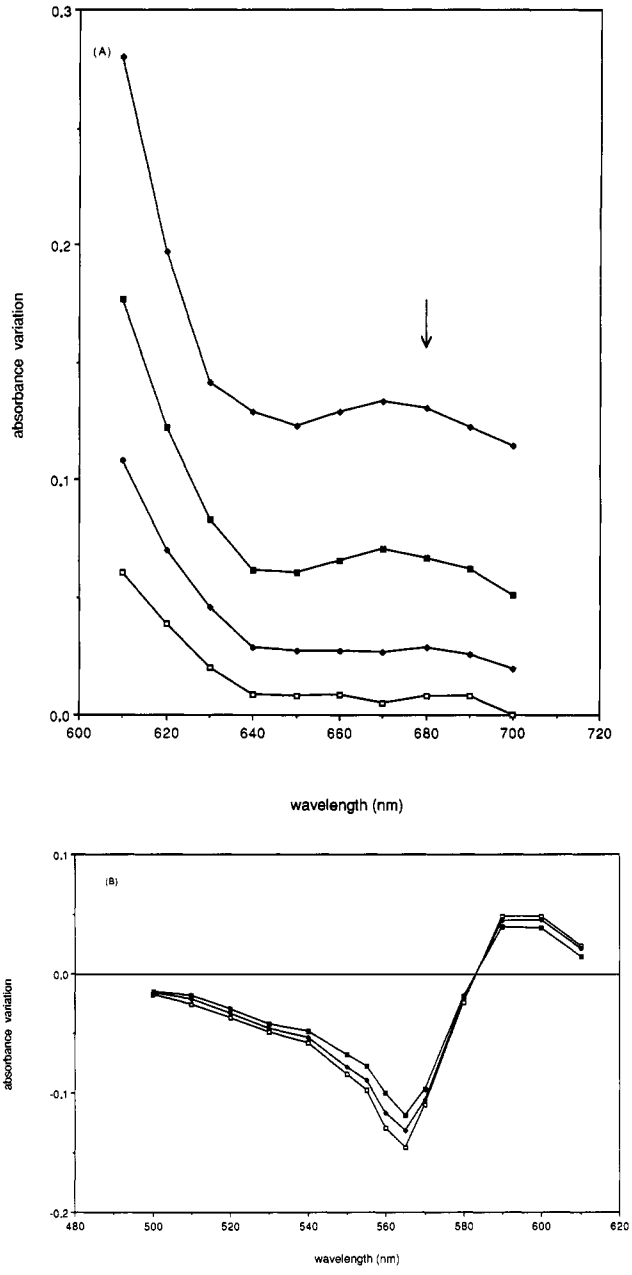

FIGURE 3: Time-resolved difference absorption spectrum of N_2-saturated aqueous solutions of MC540 and 10^{-2} M C_{16}TAB (optical path 10 cm). (A) 4×10^{-6} M MC540; (◇) 0.25 ms, (■) 2 ms, (◆) 4 ms, and (□) 8 ms after the flash trigger. (B) 10^{-6} M MC540; (□) 0.5 ms, (◆) 1.5 ms, and (■) 3 ms after flash trigger. The arrow points out the analysis wavelength at which the triplet decay kinetics has been recorded.

examined. In the presence of 10^{-5} M K_3FeCN_6 or 10^{-5} M NADPH, the triplet lifetime decreased to 1.1 or 1.3 ms, respectively. The presence of the various nitroxyl radicals (TEMPO, 5-DSA, 7-DSA, 12-DSA, 16-DSA) also caused a decrease of the triplet lifetime. From the linear plots of k_T ($= 1/\tau_T$) versus quencher concentration (Figure 4), the quenching rate constant (k_q) of MC540 triplet by nitroxyl radical could be calculated. The k_q values (in square decimeters per mole per second) follow the decreasing order TEMPO (3.6×10^8) > 5-DSA (3.7×10^7) > 7-DSA (3.6×10^6) > 12-DSA (2.1×10^6) > 16-DSA (1.4×10^6).

Nitroxide Photodestruction Rate in C_{12}TAB, C_{14}TAB, and C_{16}TAB. As shown in Figure 4, TEMPO and *n*-DSA quench the MC540 triplet state at different rate constants. To complete these results, ESR experiments were undertaken.

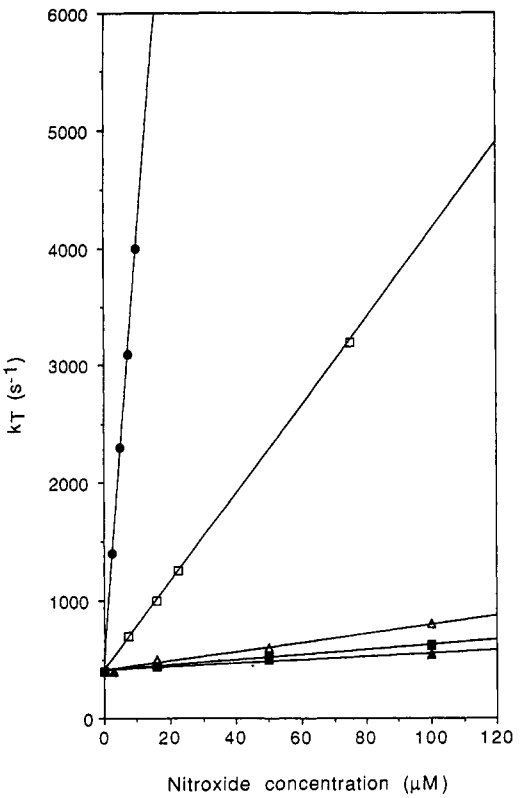

FIGURE 4: Dependence of the decay rate constant of MC540 triplet versus nitroxide concentrations in N_2-saturated aqueous solution containing 10^{-2} M C_{16}TAB and 4×10^{-6} M MC540. (●) TEMPO, (□) 5-DSA, (△) 7-DSA, (■) 12-DSA, and (▲) 16-DSA.

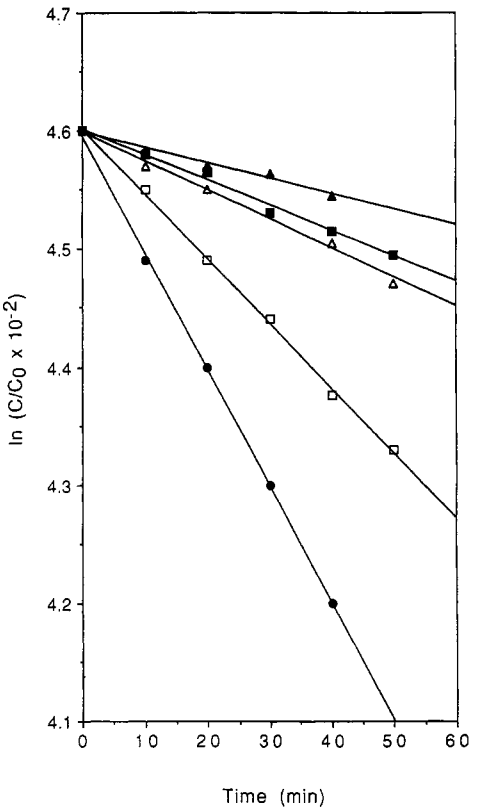

FIGURE 5: Reduction of *n*-DSA concentration mediated by MC540 (8×10^{-5} M) in N_2-saturated aqueous solutions containing 10^{-2} M C_{16}TAB as a function of the illumination time. C and C_0 (6×10^{-5} M) are the nitroxide concentration during the irradiation and the nitroxide concentration before irradiation, respectively. (▲) 16-DSA, (■) 12-DSA, (△) 7-DSA, (□) 5-DSA, and (●) TEMPO.

Under anaerobic conditions, the irradiation with visible light of MC540 (8×10^{-5} M) and *n*-DSA (6×10^{-5} M) solubilized in C_{16}TAB micelles led to the decrease of the ESR nitroxide signal amplitude (Figure 5). The corresponding destruction rates constant followed the decreasing order TEMPO > 5-DSA > 7-DSA > 12-DSA > 16-DSA. It is interesting to note that k_q values determined by flash photolysis followed the same decreasing order. Irrespective of the situation encountered in the liposomes (Figure 2), the photodestruction rate of 16-DSA mediated by MC540 was not enhanced in these conditions.

The nitroxyl group of 5-DSA and 7-DSA being located near the micelle or the vesicle interface (Jost et al., 1971), all these results suggested that a maximal photodestruction rate was obtained near the micelle or the vesicle interface. Indeed, in heterogenous systems containing amphiphilic molecules, the stearic acid nitroxide spin label was oriented parallel to the amphiphilic components (Bales & Leon, 1978; Bales & Kevan, 1982). However, a flexibility gradient was observed in the liposome system, allowing the C_{16} nitroxide to make frequent excursions toward the bilayer surface entering the region of the membrane occupied by the spin-label located at C_5 (Feix et al., 1984). In order to study the influence of these effects, we have used surfactants with decreasing chain length to change the C_{16} nitroxide group location with respect to micellar interface. Table I reports the rate constants of the decrease of the 5-, 7-, 12- and 16-DSA ESR signal amplitude in C_{16}TAB (10^{-2} M), in C_{14}TAB (1.2×10^{-2} M), and in C_{12}TAB (2×10^{-2} M) aqueous solution induced by MC540 irradiated with visible light under anaerobic conditions. Surfactant concentration was adapted to obtain identical micelle concentration with the three alkylammonium bromides (see Experimental Procedures). Using constant MC540 (8×10^{-5} M) and *n*-DSA (6×10^{-5} M) concentrations, the MC540 and *n*-DSA to micelle concentration ratios were kept constant throughout these experiments. In comparison with C_{16}TAB micelles, the photodestruction rate constant of 16-DSA became similar to that of 12-DSA in the C_{14}TAB micelles. In C_{12}TAB micelles, the photodestruction rate constant of 16-DSA intercalated between those of 7-DSA and 12-DSA, as in liposomes. Therefore, the vertical fluctuation of the probe, brought about here artificially by the use of a shorter surfactant chain, could significantly influence the reduction rate of 16-DSA spin label.

Table I: Rate Constants of the Decrease of the *n*-DSA ESR Signal Amplitude in C_{16}TAB, C_{14}TAB, and C_{12}TAB Micelles

	C_{16}TAB (min^{-1})	C_{14}TAB (min^{-1})	C_{12}TAB (min^{-1})
5-DSA	5.5×10^{-3}	1.0×10^{-2}	2.2×10^{-2}
7-DSA	2.5×10^{-3}	6.5×10^{-3}	2.0×10^{-2}
12-DSA	2.2×10^{-3}	5.5×10^{-3}	1.2×10^{-2}
16-DSA	1.3×10^{-3}	5.2×10^{-3}	1.7×10^{-2}

DISCUSSION

The ESR spectrum of *n*-DSA is sensitive to the rotational mobility of the spin label. By varying the position of the nitroxide group along the chain of a lipid spin label, it is possible to examine the lipidic structure of liposomes at various depths (Leterrier et al., 1976). The location of nitroxide stearic acid in the bilayers has been studied by others. It is well established that 5-DSA and 7-DSA explore the polar part while 12- and 16-DSA explore the hydrophobic core (Smith, 1972). The mean distance between the fatty acid carboxyl carbon and the carbon atom to which the doxyl group is bound has been calculated assuming that the molecule is linear and rigidly

extended. It is about 8, 10.5, 17, and 21.5 Å for 5-, 7-, 12-, and 16-DSA, respectively (Jost et al., 1971). The ESR spectra depicted in Figure 1 and the calculated τ_c and S values (see Experimental Procedures) are in good agreement with previous results showing that the lipidic polar zone of the liposome is rigid and relatively highly ordered whereas the hydrophobic core is fluid (Henry & Keith, 1971; Yoshioka, 1978; Takahashi et al., 1988). In micelles, a reasonable assumption is that the *n*-DSA are organized similarly to the surfactant molecules themselves with their carboxyl head group in the region of the polar head group of these molecular assemblies. The nitroxide label would be deeper into the micelle, on average, the higher the value of *n* (Bales & Kevan, 1982; Scaiano & Paraskevopoulos, 1984; Szajdzinska-Pietek et al., 1984; Baglioni et al., 1990a; 1990b).

Under irradiation with visible light, MC540 can lead to the disappearance of the nitroxide in ethanolic solution (Figure 2). This destruction is not affected by N_2O bubbling. Therefore the participation of a photoejected electron in the destruction mechanism of the label can be ruled out. Also the Type 1 pathway cannot be attributed to a photoaddition mechanism since the shape of the ESR signal remains unaffected during the experiment. Moreover, it is unlikely that the photoprocess involves directly the lowest excited singlet state of MC540 as a reactive intermediate since the addition of nitroxide spin labels leaves the fluorescence emission spectrum MC540 unchanged. The presence of oxygen in the solution during irradiation decreases considerably the destruction rate of the spin label. This observation indicates that MC540 triplet state could be implicated in the ESR signal loss. Indeed, in the presence of oxygen, a competition between the inhibition of MC540 triplet state by the nitroxide and by oxygen would be expected and would slow down the spin label destruction rate. This competition could explain the slowing down of spin label destruction in the presence of oxygen. In order to study deeply the role of the MC540 triplet state in the process, flash photolysis experiments have been performed in C_{16}TAB micelles. The examination of Figure 4 reveals clearly that the lifetime of the dye triplet state is reduced by the presence of TEMPO and all *n*-DSA, in a concentration-dependent fashion. These results shed more light on the direct participation of MC540 triplet state in nitroxide destruction.

However, it is not possible to conclude on the precise reaction initiated by the triplet. Indeed, the reaction could be an electron transfer from the MC540 triplet state to the spin label. Such a transfer has been observed, in ethanol, between carbocyanine molecules having two polymethine chains and nitroxides (Kuzmin et al., 1978). Another possibility could be a reaction between nitroxides and MC540 radicals (Feix & Kalyanaraman, 1991). Indeed, radical anion ($MC^{\bullet -}$) and radical cation ($MC^{\bullet +}$) of MC540 are likely to be generated by the quenching of MC540 triplet state (^3MC) by MC540 ground state (MC) (Feix & Kalyanaraman, 1991):

$$^3MC + MC \rightarrow MC^{\bullet +} + MC^{\bullet -} \quad (1)$$

Using ESR and flash photolysis, it has been shown that $MC^{\bullet -}$ and $MC^{\bullet +}$ absorb in methanol around 400 and 420 nm, respectively (Sarna et al., 1990, 1991; Davila et al., 1991; Harriman et al., 1991). Therefore, we have attempted to detect their formation after excitation of MC540 and *n*-DSA or TEMPO solutions. No signal could be detected in the 400-nm wavelength region whatever the flash intensity or the nitroxyl radical concentration. However, these experiments could not be considered as conclusive. Indeed, using electron donor NADPH or electron acceptor $K_3Fe(CN)_6$, quenching of MC540 triplet state was observed, but again no transient absorption in the 400–420-nm region could be detected. These results could be interpreted by either a too weak production yield of radicals or a fast recombination process promoted by the micelle (charge and proximity effects) leading to radical lifetimes lower than the resolution time of our flash photolysis apparatus. However, it can be stressed that the involvement of the $MC^{\bullet -}$ and $MC^{\bullet +}$ forms in the *n*-DSA or TEMPO destruction seems to be unlikely. Such a suggested pathway would imply a second-order reaction in MC540 concentration. This hypothesis does not fit with the ESR experiments carried out in ethanol. Indeed, the spin label destruction rate constant is first-order dependent on dye concentration.

When the nitroxide free radicals are incorporated as spin labels inside micelles or lipidic structures like DMPC liposomes, the kinetics of their paramagnetic signal decay under irradiation in the presence of MC540 gives also information about the MC540 location inside the structure. Our results in DMPC liposomes clearly indicate, in disagreement with those published by Feix and Kalyanaraman (1991), that the rates of spin label destruction are influenced by the position of the nitroxide group along the fatty acid chain. The main parameter responsible for the effects above is clearly the distance between the polar head group and the nitroxide group, to which a dielectric constant effect could be added. Our results have been strengthened by ESR and flash photolysis experiments, carried out in aqueous micelles, which have shown up a similar effect. In C_{16}TAB, both ESR and flash photolysis data show that TEMPO is generally more reactive than the doxyl derivatives (see Figures 4 and 5). The more efficient reaction could reflect a higher mobility of TEMPO resulting from the absence of a long hydrophobic chain (Scaiano & Paraskivopoulos, 1984). The higher quenching rate constant for 5-DSA compared with 7-DSA, 12-DSA, and 16-DSA should also be the result of a better micellar surface access by the former.

In liposomes, our data (Figure 2) show that fastest rates of ESR signal photoreduction are observed with 5-DSA, whose nitroxyl radical is close to the surface, and with 16-DSA, having its nitroxyl radical embedded deeply in the membrane. Previous studies have shown that a monomer–dimer equilibrium exists within the lipid bilayer membrane and there is a 5-fold excess of MC540 monomers which are oriented parallel to the phospholipid chains with their sulfonated groups near the membrane surface over those oriented in the perpendicular direction (Verkman, 1987). The dimers are located deeply within the membrane, perpendicular to the phospholipid chains. Our results suggest that MC540 monomers which are oriented parallel to the phospholipid chains interact preferentially with nitroxyl groups situated at the level of the C_5 position, near the membrane surface. Since MC540 is a long molecule of about 16 Å (Verkman, 1987), the high efficiency for 16-DSA photoreduction, in which the nitroxide group is situated more deeply in the hydrophobic core (Jost et al., 1971), leads us to suspect that the monomers or the dimers or both, oriented perpendicularly to the phospholipid chain, could be responsible for the destruction of 16-DSA radical nitroxide. However, 16-DSA is also able to undergo vertical fluctuations in the liposomal membrane, reflecting flexibility of the fatty acid alkyl chain (Feix et al., 1984). In Table I is shown the variation of the ESR signal reduction rate constants of the doxyl stearic acids when the surfactant chain length decreases. When the surfactant chain is short (i.e., C_{12}TAB), the stearic acid chain is probably bent, the C_{16} nitroxide coming close to the level of the micelle occupied

usually by C_5 (Baglioni et al., 1990a,b). Consequently, the vertical fluctuations of the probe could be another explanation for the increased efficiency for the 16-DSA reduction.

In conclusion, we have shown that photoexcited MC540 is able to destroy the paramagnetism of spin-labeled doxyl stearic acid incorporated in micelle or in liposome by a Type 1 mechanism. The MC540 triplet state seems to be directly implicated in the reaction process while the singlet state is not. Our results demonstrate clearly that the kinetics of destruction of *n*-DSA in micelles and unilamellar liposomes are affected by the position of the doxyl moiety along the stearic acid chain.

REFERENCES

Abu-Hamdiyyah, M., & Kumari, K. (1990) *J. Phys. Chem. 94*, 2518–2523.

Aramendia, P. F., Krieg, M., Nitsch, C., Bittermann, E., & Braslavsky, S. E. (1988) *Photochem. Photobiol. 48*, 187–194.

Baglioni, P., Hu, M., & Kevan, L. (1990a) *J. Phys. Chem. 94*, 2586–2590.

Baglioni, P., Hu, M., & Kevan, L. (1990b) *J. Phys. Chem. 94*, 8218–8222.

Bales, B. L., & Leon, V. (1978) *Biochim. Biophys. Acta 90*, 509–517.

Bales, B. L., & Kevan, L. (1982) *J. Phys. Chem. 86*, 3836–3839.

Chapman, D., Williams, R. M., & Ladbrooke, B. D. (1967) *Chem. Phys. Lipids 1*, 445–450.

Chen, K., Morse, P. D., & Swartz, H. M. (1988) *Biochim. Biophys. Acta 943*, 477–484.

Chen, K., Glockner, J. F., Morse, P. D., & Swartz, H. M. (1989) *Biochemistry 28*, 2496–2501.

Davila, J., Gullija, K. S., & Harriman, A. (1989) *J. Chem. Soc., Chem. Commun.*, 1215–1216.

Davila, J., Harriman, A., & Gulliya, K. S. (1991) *Photochem. Photobiol. 1*, 1–11.

Dodin, G., Aubard, J., & Falque, D. (1987) *J. Phys. Chem. 91*, 1166–1172.

Dousset, N., Ferre, G., Massol, M., & Douste-Blazy, L. (1986) *Arch. Biochem. Biophys. 246*, 716–724.

Feix, J. B., & Kalyanaraman, B. (1991) *Photochem. Photobiol. 53*, 39–45.

Feix, J. B., Popp, C. A., Venkataramu, S. D., Beth, A. H., Park, J. H., & Hyde, J. S. (1984) *Biochemistry 23*, 2293–2299.

Ferradini, C. (1986) *Biochimie 68*, 779–785.

Harriman, A., Shoute, L. C. T., & Neta, P. (1991) *J. Phys. Chem. 95*, 2416–2420.

Henry, S., & Keith, A. (1971) *Chem. Phys. Lipids 7*, 245–265.

Hoebeke, M., Seret, A., Piette, J., & Van de Vorst, A. (1988) *J. Photochem. Photobiol. 1*, 437–446.

Hoebeke, M., Piette, J., & Van de Vorst, A. (1990) *J. Photochem. Photobiol., B 4*, 273–282.

Hoebeke, M., Piette, J., & Van de Vorst, A. (1991) *J. Photochem. Photobiol., B 9*, 281–294.

Hope, M. J., Bally, M. B., Webb, G., & Cullis, P. R. (1985) *Biochim. Biophys. Acta 812*, 55–65.

Hubbel, W. L., & Mc Connell, H. M. (1971) *J. Am. Chem. Soc. 93*, 314–326.

Imae, T., Abe, A., Taguchi, Y., & Ikeda, S. (1986) *J. Colloid Interface Sci. 109*, 567–575.

Jost, P., Libertini, L. J., Hebert, V. C., & Griffith, O. H. (1971) *J. Mol. Biol. 59*, 77–98.

Kalyanaraman, B., Feix, J. B., Sieber, F., Thomas, J. P., & Girotti, A. W. (1987) *Proc. Natl. Acad. Sci. U.S.A. 79*, 2999–3003.

Kuzmin, V. A., Tatikolov, A. S., & Boriscvich, Yu. E. (1978) *Chem. Phys. Lett. 53*, 52–54.

Leterrier, F., Mendyk, A., & Viret, J. (1976) *Biochem. Pharmacol. 25*, 2469–2474.

Mayer, L. D., Hope, M. J., & Cullis, P. R. (1986) *Biochim. Biophys. Acta 858*, 161–168.

Melhorn, R. J., & Packer, L. (1982) *Can. J. Chem. 60*, 1452–1462.

Nayar, R., & Schroit, A. J. (1985) *Biochemistry 24*, 5967–5971.

Pryor, W. A. (1976) in *Free Radicals in Biology* (Pryor, W. A., Ed.) Vol. 1, pp 1–43, Academic Press, New York.

Sarna, T., Pilas, B., Lambert, C., Land, E. J. & Truscott, T. G. (1990) *Photochem. Photobiol. 51*, 42S.

Sarna, T., Pilas, B., Lambert, C., Land, E. J., & Truscott, T. G. (1991) *J. Photochem. Photobiol., A 58*, 339–347.

Scaiano, J. C., & Paraskevopoulos, C. I. (1984) *Can. J. Chem. 62*, 2351–2354.

Seret, A., & Van de Vorst, A. (1990) *J. Phys. Chem. 94*, 5293–5299.

Seret, A., Hoebeke, M., & Van de Vorst, A. (1990) *Photochem. Photobiol. 52*, 601–604.

Sieber, F., Craig, A., Krueger, G. J., Smith, R. E., & Ash, R. C. (1986) *Blood 86*, 292A.

Sieber, F., Stuart, R. K., Rowley, S. D., Sharkis, S. J., & Sensenbrenner, L. L. (1987a) *Leukemia 11*, 43–50.

Sieber, F., O'Brien, J. M., Krueger, G. J., Schober, S. L., Burns, W. H., Sharkis, S. J., & Sensenbrenner, L. L. (1987b) *Photochem. Photobiol. 46*, 707–711.

Sikurova, L., Frankova, R., & Chovat, D. (1989) *Stud. Biophys. 133*, 163–168.

Smith, I. C. P. (1972) in *The spin label method, in biological applications of electron spin resonance* (Swartz, H. M., Bolton, J. R., & Borg, D. C., Eds.) pp 483–539, Wiley Interscience, New York.

Szajdzinska-Pietek, E., Maldonado, R., Kevan, L., & Jones, R. R. M. (1984) *J. Am. Chem. Soc, 106*, 4675–4678.

Takahashi, M., Tsuchiya, J., Niki, E., & Urano, S. (1988) *J. Nutr. Sci. Vitaminol. 34*, 25–34.

Verkman, A. S. (1987) *Biochemistry 26*, 4050–4056.

Yoshioka, H. (1978) *Colloid Interface Sci. 66*. 352–354.

Zielinski, R., Ikeda, S., Nomura, H., & Kato, S. (1988) *J. Colloid Interface Sci. 129*, 175–184.